

# Zero-Voltage Switching for Bidirectional Buck/Boost Converter using Hybrid Discontinuous Current Mode

Hoai Nam Le, Koji Orikawa, Jun-ichi Itoh

Nagaoka University of Technology

1603-1 Kamitomioka Town

Nagaoka City, Niigata Prefecture, Japan

Tel.: +81 / (258) – 47.9533.

E-Mail: lehoainam@stn.nagaokaut.ac.jp

URL: <http://itohserver01.nagaokaut.ac.jp/itohlab/index.html>

**Abstract**— This paper proposes a hybrid current mode between Triangular current mode (TCM) and Discontinuous current mode (DCM) in order to achieve Zero-voltage switching (ZVS) for a bidirectional buck/boost DC-DC converter. In the proposed Hybrid Discontinuous Current Mode entitled HDCM, the TCM operation is applied during the zero-current interval of DCM. Therefore, both ZVS and the variable current ripple, which result in the high efficiency at wide load range, are achieved. The achievement of ZVS with HDCM is confirmed by a 600-W prototype. Compared to TCM, the Root-Mean-Square current is reduced by 47.2% at most with HDCM, which further contributes to the loss reduction. Moreover, under the condition of the same boost inductor, the efficiency of HDCM at load of 0.2 p.u. is improved by 1.5% compared to TCM.

**Keywords**— Zero-voltage switching; High power density; Discontinuous current mode; Triangular current mode

## I. INTRODUCTION

Over the past decades, the increase of the power density has been one of the most important design criteria in power electronics [1]. The minimization of the converters provides not only the material cost reduction but also the easy implementation for applications which require space-saving power systems such as, e.g. Hybrid electric vehicles or Photovoltaic systems. The boost inductor is one of the components which contributes mainly to the converter volume. By increasing the switching frequency, the volume of the boost inductor can be reduced. However, higher switching frequency leads to the increase of the switching loss, which requires larger heat sinks. Therefore, the reduction of the switching loss is crucial to the high power density design.

The soft switching technique can reduce greatly the switching loss, in which the resonance between the inductor and the capacitor is utilized in order to achieve the Zero-voltage switching (ZVS). However, in order to satisfy the condition for ZVS, these methods suffer many drawbacks; e.g. the requirement of the additional components [2], or the restriction of the controllable duty ratio [3]-[4]. Consequently, the additional components not only restricts the minimization of the converter but also complicates the control

method, whereas the restriction of the voltage ratio or the duty ratio limits the application of ZVS. Therefore, the achievement of ZVS without additional components or the limited duty ratio is desired.

On the other hand, ZVS can be achieved with an advanced modulation technique, entitled Triangular current mode (TCM) [5]-[7]. In particular, in Continuous current mode (CCM), the free-wheeling diodes suffer from significant reverse recovery losses. The reverse recovery issues can be alleviated by operating the converter in Discontinuous current mode (DCM). Nevertheless, in DCM, it is still necessary to deal with two kinds of switching loss; the high turn-off loss because the switching devices are turned off at least twice of the average current, and the turn-on loss due to the junction capacitor charge. In TCM, the turn-off loss can be decreased greatly by connecting a snubber capacitor in parallel with the switching devices, whereas the turn-on loss is eliminated by ZVS. As a result, the switching frequency can be pushed to several MHz due to almost no switching loss. One of the main drawbacks in the TCM operation is that the high current ripple is constant at all load range. As a result, it is difficult to achieve high efficiency at light load when the average current is low [5]. Therefore, it is desired to reduce the current ripple at light load in order to avoid the sharp decrease in the efficiency.

This paper proposes a novel concept of the hybrid current mode between TCM and DCM, which is entitled Hybrid Discontinuous current mode (HDCM), in order to achieve both ZVS and the variable current ripple. In the proposed current mode, the TCM operation is applied during the zero-current interval of the DCM current in order to generate the condition for ZVS. As a result, this current mode can achieve the high efficiency at wide load range without additional components. This paper is organized as follows; first, the mechanism of the ZVS achievement in HDCM is described and the control method of HDCM is explained. Next, the principle operation of HDCM is confirmed by experiments and the comparison of the Root-Mean-Square (RMS) current between TCM and HDCM is conducted. Finally, the efficiency between TCM and HDCM is compared in order to confirm the effectiveness of HDCM.

## II. HYBRID CURRENT MODE BETWEEN DISCONTINUOUS CURRENT MODE AND TRIANGLE CURRENT MODE

Fig. 1 depicts the bidirectional buck/boost converter. In order to minimize the passive components, i.e. the boost inductor  $L$  and the output capacitor  $C$ , the switching frequency is required to be pushed to hundreds of kHz or even to several MHz. Hence, the switching loss reduction is crucial to the high power density design. There are three conventional current modes to operate the bidirectional buck/boost converter: CCM, DCM and TCM. Note that the Critical Current Mode (CRM) operation can be analyzed as same as the DCM operation without the occurrence of the zero-current period.

Fig. 2 illustrates the pattern of the switching losses in each current mode. In CCM shown in Fig. 2(a), the significant reverse recovery loss occurs at the beginning of the interval 1, because the free-wheeling diode FWD<sub>2</sub> is forcefully turned off. In DCM shown in Fig. 2(b), due to the natural turn-off of the free-wheeling diode FWD<sub>2</sub> at the end of the interval 4, the reverse recovery loss does not occur. Nevertheless, the junction capacitor discharges through the switch FET<sub>1</sub> at the beginning of the interval 1 in Fig. 2(b), which results in the hard switching. On the other hand, in TCM shown in Fig. 2(c), the current commutates from the switch FET<sub>2</sub> to the free-wheeling diode FWD<sub>1</sub> during the interval 4, and gradually discharges the junction capacitor. Hence, the switch FET<sub>1</sub> is turned on at the forward voltage of the free-wheeling diode FWD<sub>1</sub>, which is considered as ZVS. As a conclusion, the principle of the ZVS achievement in TCM is to flow a negative current in order to discharge the junction capacitor. Besides, it should be noted that the turn-off loss can be reduced simply by connecting a snubber capacitor in parallel with the switch [7]. However, a drawback of TCM is the large current ripple which decreases notably the efficiency at light load. Therefore, the current ripple reduction of TCM at light load is desired.

In order to reduce the current ripple, one of the conventional methods is to increase the switching frequency at light load, i.e. the Pulse Frequency Modulation (PFM) [6]. However, PFM is undesirable in many power electronic systems because it is difficult to design a filter circuit for the operation across a wide range of frequencies. On the other hand, in the DCM operation, because the current ripple becomes smaller at light load, the high efficiency can be maintained. As mentioned above, because the DCM operation still suffers the high turn-on loss, the method to achieve ZVS in DCM is desired. Therefore, this paper proposes the novel concept where TCM and DCM are combined in order to utilize the advantage of both TCM and DCM, i.e. ZVS in TCM and the current ripple reduction at light load in DCM.

Fig. 3 illustrates the concept of the hybrid current mode (HDCM) between DCM and TCM. During the zero-current interval in DCM, i.e. the interval 4 and 5 in Fig. 2(b), instead of let the current return to zero, the switches are modulated in order to flow the TCM current. As a result, the condition in order to achieve ZVS in the DCM operation can be satisfied by the TCM current during the interval 4 in Fig. 3. Note that the switching losses during the TCM operation are negligibly small as explained above. Further-

more, because the total charge during the TCM interval can

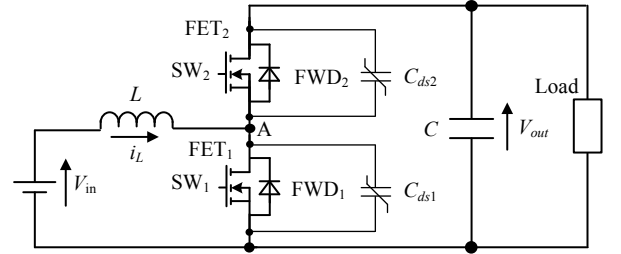
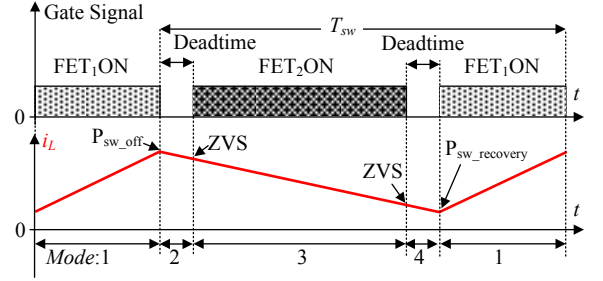
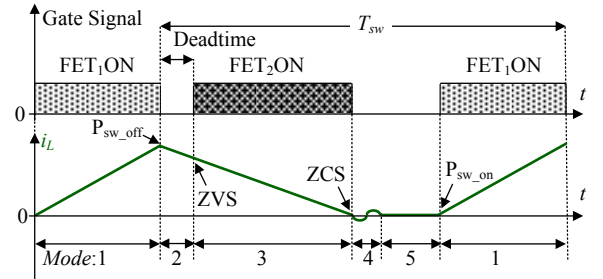


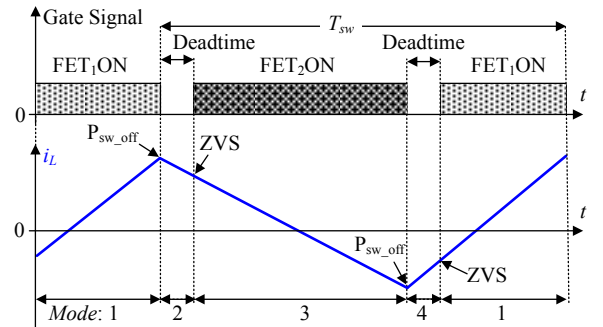
Fig. 1. Bidirectional buck/boost DC-DC converter. The switching loss reduction is crucial to the high power density design. In general, there are three current modes to operate the converter: CCM, DCM and TCM.



(a) Switching losses in CCM. In the CCM operation, the free-wheeling diodes suffer from significant reverse recovery losses.



(b) Switching losses in DCM. The reverse recovery issues can be alleviated by DCM. Nevertheless, in the DCM operation, two kinds of switching loss still occur; the high turn-off loss because the switching devices is turned off at least twice of the average current, and the turn-on loss due to the junction capacitor charge of the free-wheeling diodes.



(c) Switching losses in TCM.

Fig. 2. Switching losses in CCM, DCM and TCM. In the TCM operation, the turn-off loss can be decreased greatly by connecting a snubber capacitor in parallel with the switching devices, whereas the turn-on loss is eliminated by ZVS by using the inductor to resonate out the junction capacitor charge [6]. By utilizing TCM, ZVS is achieved without additional components or the limited duty ratio. However, the high current ripple is constant at all load range, which results in the shape decline of the efficiency at light load.

be controlled to become negligibly small, the TCM interval is considered to have no effects on the DCM operation. On the other words, the current ripple at light load can be reduced by the DCM operation. Consequently, both ZVS and the current ripple reduction at light load are achieved without additional components or the limited duty ratio.

### III. CONTROL OF HYRID DISCONTINUOUS CURRENT MODE

Because HDCM is combined of two current modes, i.e. DCM and TCM, the DCM feedback current control and the TCM switching pulse generation are introduced. In particular, the DCM nonlinearity which occurs in the duty-ratio-to-current transfer function due to the zero-current interval, worsens the current control performance if the same PI controller is applied as in CCM [8]-[10]. Therefore, in this section, first, the current feedback control with the DCM nonlinearity compensation is introduced. Next, the generation of the duty cycles for the TCM operation during the zero-current interval is explained.

#### A. Discontinuous current mode feedback current control

Fig. 4 depicts the inductor current waveform in DCM, where  $D_1$ ,  $D_2$  and  $D_0$  denote the duty ratios of the first, the second and the zero-current interval. Note that the output voltage  $V_{out}$  is assumed to be constant in the design step of the feedback current control because the inductor current response is generally designed to be much faster than the output voltage response. The equation based on the average model of the boost/buck converter in DCM is given by (1),

$$L \frac{di_{L\_avg}}{dt} = D_1 V_{in} + D_2 (V_{in} - V_{out}) \dots \dots \dots (1)$$

where  $V_{in}$  is the input voltage. The average current  $i_{L\_avg}$  and the current peak  $i_{L\_peak}$ , which are shown in Fig. 4 are expressed as,

$$i_{L\_avg} = \frac{i_{L\_peak}}{2} (D_1 + D_2) \dots \dots \dots (2)$$

$$i_{L\_peak} = \frac{V_{in}}{L} D_1 T_{sw} \dots \dots \dots (3)$$

where  $T_{sw}$  is the switching period. Substituting (3) into (2) and then solving the equation for the duty ratio  $D_2$ . The duty ratio  $D_2$  is expressed by (4),

$$D_2 = \frac{2L i_{L\_avg}}{D_1 T_{sw} V_{in}} - D_1 \dots \dots \dots (4)$$

Substituting (4) into (1) in order to remove the duty ratio  $D_2$  and represent (1) as a function of only the duty ratio  $D_1$ , then (5) is obtained [8],

$$L \frac{di_{L\_avg}}{dt} = V_{in} - V_{out} + D_1 V_{out} + (V_{out} - V_{in}) \left(1 - \frac{2L i_{L\_avg}}{V_{in} D_1 T_{sw}}\right) \dots \dots \dots (5)$$

Next the duty-ratio-to-current transfer function in DCM  $G_{i\_DCM}$  is obtained by linearizing (5) at the steady-state operating points [9],

$$G_{i\_DCM}(s) = \frac{\Delta i_{L\_avg}(s)}{\Delta D_1(s)} = \frac{2V_{dc}}{sL + \frac{2(V_{out} - V_{in})L}{V_{in} D_{1s} T_{sw}}} \dots \dots \dots (6)$$

where  $\Delta i_{L\_avg}$  and  $\Delta D_1$  are the small signals of the average current  $i_{L\_avg}$  and the duty ratio  $D_1$ , and  $D_{1s}$  is the duty ratio of SW<sub>1</sub> at the steady-state operating points. On the other hand, the duty-ratio-to-current transfer function in CCM was derived in [9], yielding

$$G_{i\_CCM}(s) = \frac{\Delta i_{L\_avg}(s)}{\Delta D_1(s)} = \frac{V_{dc}}{sL} \dots \dots \dots (7)$$

Fig. 5 shows the gain of the duty-ratio-to-current transfer function in CCM and DCM under different conditions of the steady-state duty-ratio  $D_{1s}$ . In most cases, the frequency corresponding to the pole of  $G_{i\_DCM}$  is certainly much higher than the cutoff frequency of the current control loop  $f_n$ . Consequently, the open loop gain in DCM is much lower than in CCM. This worsens the current response in DCM if the same PI controller as in CCM is employed in DCM. Therefore, the output of PI controller is necessary to be compensated when the circuit is operated in DCM in order to achieve the same current command response as in CCM.

Fig. 6 illustrates the circuit model of the buck converter in the DCM operation which is based on (6). In CCM, the dash line part does not exist, because the average current  $i_{L\_avg}$  equals to the half current peak  $i_{L\_peak}/2$ . On the other words, this makes the zero-current interval  $D_0 T_{sw}$  in Fig. 5 become zero. However, in DCM, the voltage at point A in Fig. 4 occurring during the zero-current interval introduces the nonlinearity into the DCM transfer function. In order to design of the compensation part for the nonlinearity of DCM, the circuit model in Fig. 7 is linearized at the steady-state operating points.



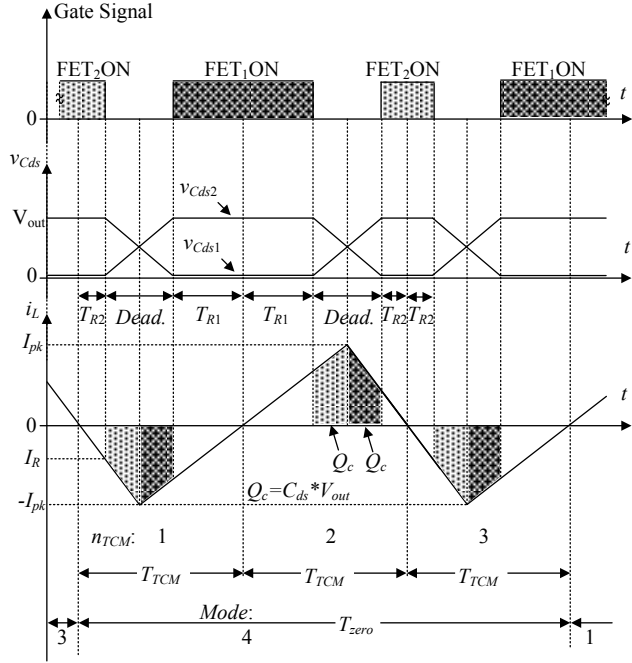


Fig. 9. Flowchart of switching signal generation during TCM interval. In order to achieve ZVS for the DCM operation, the TCM period  $T_{TCM}$  is adjusted according to the zero-current period  $T_{zero}$ . Furthermore, in order to minimize the losses from the additional TCM current, the current peak  $I_{pk}$  is designed to be just large enough to achieve ZVS for both switches  $SW_1$  and  $SW_2$  during the TCM interval. Finally, in order to make the TCM interval have no influence on the DCM operation, which implies the total charge from the additional TCM current is negligibly small, the positive and negative values of the current peak  $I_{pk}$  is controlled to be the same.

Fig. 9 illustrates the waveforms of the gate signal, the junction capacitor voltage and the current during the TCM interval in case of  $V_{in} > V_{out}/2$ . First, the minimum current peak  $I_{pk\_min}$  which achieves the condition of ZVS for  $SW_1$  is calculated from the total charge stored  $Q_c$  in the junction capacitor  $C_{ds}$  as in [6], yielding

$$I_{pk\_min} = \sqrt{\frac{2C_{ds}V_{out}V_{in}}{L}} \quad (8)$$

In order to let the inductor current reach the peak  $I_{pk\_min}$ , the required TCM period  $T_{TCM\_min}$  is calculated by (9),

$$T_{TCM\_min} = I_{pk\_min} L \left( \frac{1}{V_{out} - V_{in}} + \frac{1}{V_{in}} \right) \quad (9)$$

Next, the number of the TCM period  $n_{TCM}$  is calculated from the zero-current period  $T_{zero}$  which is shown as  $D_0 T_{sw}$  in Fig. 4. The zero-current period  $T_{zero}$  is estimated from the duty ratio of  $SW_1$  which is generated from the current control in Fig. 7, yielding

$$T_{zero} = T_{sw} \left( 1 - D_1 \frac{V_{out}}{V_{out} - V_{in}} \right) \quad (10)$$

In order to minimize the losses from the TCM interval, the current peak  $I_{pk}$  of the TCM current is required to be minimal. Consequently, it is necessary to choose the number of the TCM period  $n_{TCM}$  as a maximum odd number, yielding

Input Voltage	$V_{in}$	150 V
Output Voltage	$V_{out}$	285 V
Rated Power	$P_n$	600 W
Switching Frequency	$f_{sw}$	100 kHz
Dead Time	$T_d$	200 ns
Boost Inductor	$L$	74 $\mu$ H
Output Capacitor	$C$	10 $\mu$ F
Switching Device: TPH3006PS		

$$n_{TCM} \leq \frac{T_{zero}}{T_{TCM\_min}}; n_{TCM} \text{ is an odd number.} \quad (11)$$

Next, the actual TCM period  $T_{TCM}$  is calculated from the zero-current period  $T_{zero}$  and the number of the TCM period  $n_{TCM}$ ,

$$T_{TCM} = \frac{T_{zero}}{n_{TCM}} \quad (12)$$

Then, the actual current peak  $I_{pk}$  of the TCM current is expressed as in (13),

$$I_{pk} = \frac{T_{TCM}}{L \left( \frac{1}{V_{out} - V_{in}} + \frac{1}{V_{in}} \right)} \quad (13)$$

Finally, the duty ratios  $T_{R1}$  and  $T_{R2}$  of  $SW_1$  and  $SW_2$  in order to achieve the TCM current peak  $I_{pk}$  is expressed as in (14) and (15), respectively [6],

$$T_{R1} = \frac{L}{V_{in}} \sqrt{I_{pk}^2 - \frac{2C_{ds}V_{out}V_{in}}{L}} \quad (14)$$

$$T_{R2} = \frac{L}{V_{out} - V_{in}} \sqrt{I_{pk}^2 - \frac{2C_{ds}V_{out}(V_{out} - V_{in})}{L}} \quad (15)$$

As shown in Fig. 9, the positive and negative values of the current peak  $I_{pk}$  is controlled to be the same, which enables the total charge from the additional TCM current to be negligibly small. Consequently, the TCM interval has almost no influence on the DCM operation.

#### IV. EXPERIMENTAL RESULTS

Table 1 shows the experimental parameters. The design of the converter with high switching frequency and high inductor current in HDCM benefits the reduction of the boost inductance. Note that the inductor is designed in order to operate the converter in TCM at rated load. Besides, the design of the output voltage control is as same as one in the CCM operation because the DCM nonlinearity is eliminated completely.

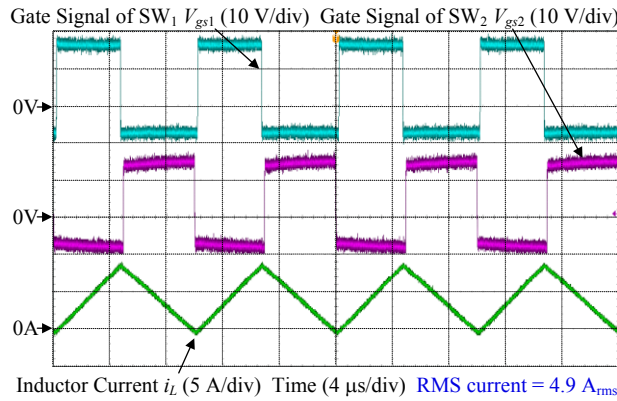
Fig. 10 depicts the waveforms of the TCM and HDCM current, the junction capacitor voltage, and the gate signal under different conditions of load. At the rated load, the current waveforms are same for both HDCM and TCM. However, at light load, compared to the TCM operation, the current ripple is greatly reduced by HDCM. In particular, at the condition of light load of 0.2 p.u., the RMS current is re-

duced from  $2.9 A_{rms}$  to  $1.5 A_{rms}$ . Furthermore, as shown in Fig. 10(d)-(e), the positive and negative values of the TCM current are controlled to be almost the same. Consequently, the addition TCM current has no effects on the DCM operation.

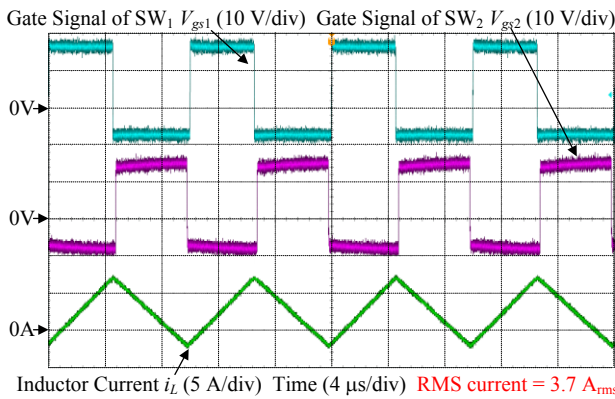
Fig. 11 illustrates the waveforms of the gate signal and the junction capacitor voltage, which is the magnified waveforms from Fig. 10(e). It is confirmed that both the switches  $SW_1$  and  $SW_2$  are turned on at the zero voltage, which result in ZVS. Furthermore, the turn-off losses can be greatly reduced by connecting a snubber capacitor parallel to the switch in order to delay the increase of the junction voltage.

Consequently, almost no switching loss can be accomplished in order to further increase the switching frequency and achieve the high power density. Note that there are no surge voltage occurring in the junction voltage of both switches  $SW_1$  and  $SW_2$  due to the achievement of soft switching.

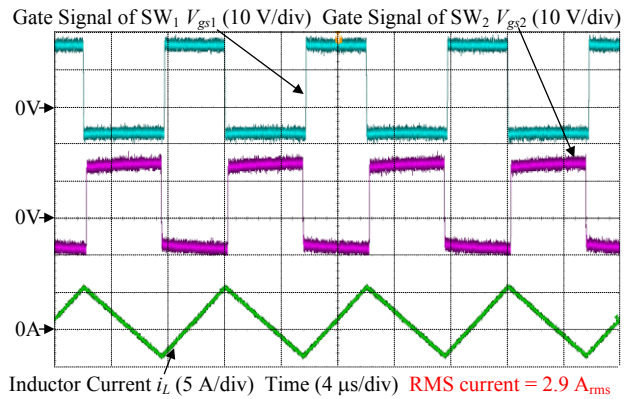
Fig. 12 illustrates the current response of HDCM. The TCM current peak  $I_{pk}$  is controlled according to the zero-current period  $T_{zero}$ , which is dependent on the average current  $i_{L\_avg}$ . Consequently, ZVS for both switches  $SW_1$  and  $SW_2$  is achieved in all load range, i.e. the ZVS achievement is unlimited by the condition of load or the duty ratio. Besides, there is a small oscillation occurring in the average



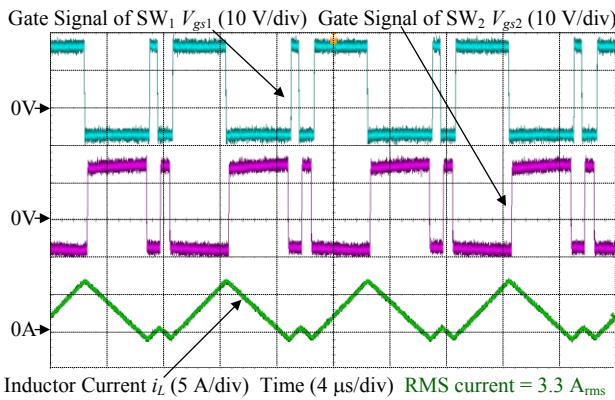
(a) TCM and HDCM current and gate signals at rated load of 1.0 p.u..



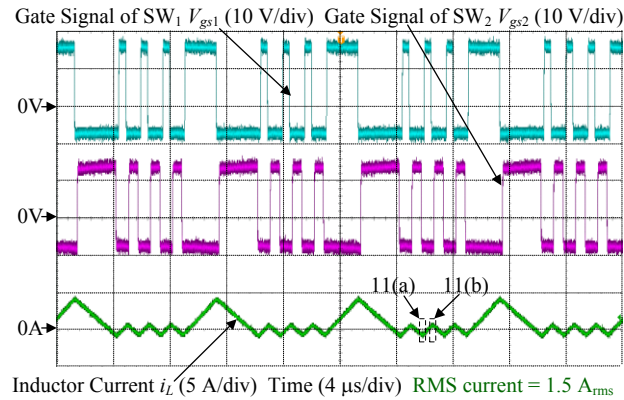
(b) TCM current and gate signals at light load of 0.6 p.u..



(c) TCM current and gate signals at light load of 0.2 p.u..



(d) HDCM current and gate signals at light load of 0.6 p.u..

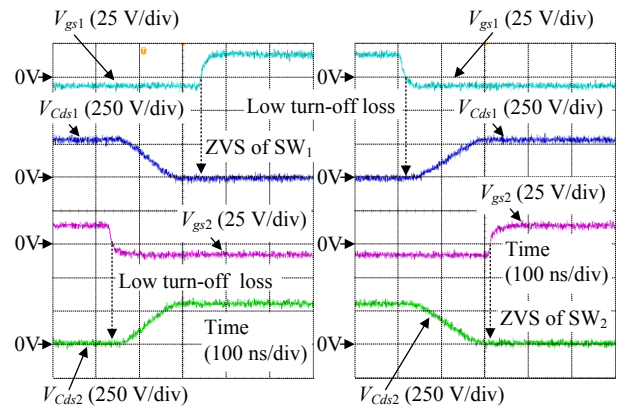


(e) HDCM current and gate signals at light load of 0.2 p.u..

Fig. 10. Waveforms of TCM and HDCM current, junction capacitor voltage, and gate signal under different conditions of load. By utilizing the characteristic of the zero-current interval in DCM, the current ripple of HDCM is reduced at light load. In particular, compared to the TCM operation, the RMS current in the HDCM operation is reduced from  $2.9 A_{rms}$  to  $1.5 A_{rms}$  at light load of 0.2 p.u..

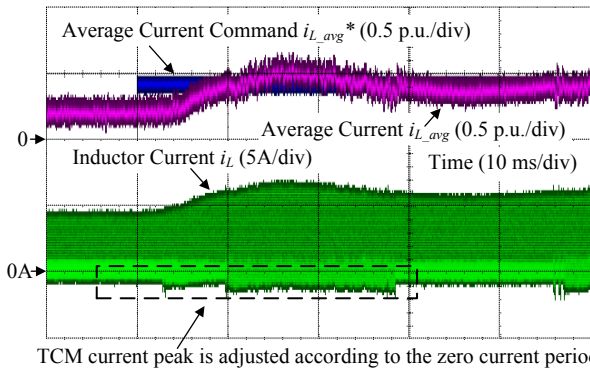
current  $i_{L\_avg}$ . This is because the sampling frequency as well as the control frequency is set as 10 kHz which is lower 10 times than the switching frequency of 100 kHz. Accordingly, this problem can be solved simply by designing the control frequency equal to the switching frequency.

Fig. 13 shows the comparison of RMS current and efficiency between TCM and HDCM. First, in the results of the ratio between the RMS current  $i_{L\_rms}$  and the average current  $i_{L\_avg}$ , by utilizing the variable current ripple of DCM, the RMS current in the HDCM operation is reduced greatly compared to the TCM operation. In particular, at light load of 0.2 p.u., the RMS current of HDCM is reduced by 47.2%. Besides, the RMS current of HDCM at rated load is as same as one in TCM, because the converter is designed to be operated with TCM at rated load. This design minimized the required current ripple in order to achieve ZVS at rated load. Consequently, the efficiency of HDCM at rated load is as same as one in TCM, whereas at light load of 0.2 p.u., the efficiency is improved by 1.5% with the HDCM operation. Therefore, by applying HDCM, the high efficiency is achieved at wide load range, which results in the high weighted efficiency of 98.8% at the switching frequency of

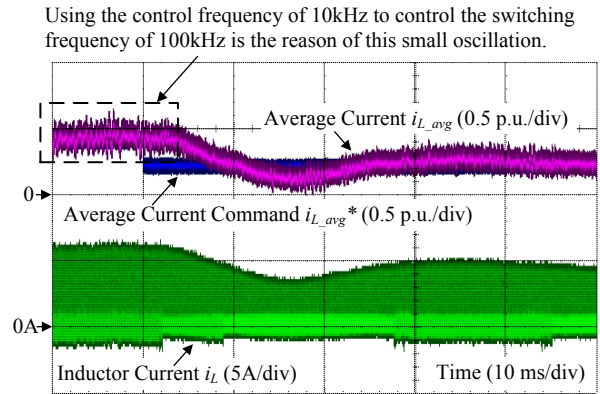


(a) ZVS of SW1. (b) ZVS of SW2.

Fig. 11. Waveforms of gate signal and junction capacitor voltage in HDCM operation which is the magnified waveforms from Fig. 10(e). By flowing the TCM current during the zero-current interval of DCM, ZVS is achieved for both switches SW<sub>1</sub> and SW<sub>2</sub>, which results in no turn-on loss. Furthermore, the turn-off loss can be greatly reduced by connecting a snubber capacitor parallel to the switch in order to delay the increase of the junction voltage  $v_{Cds1}$  and  $v_{Cds2}$ .

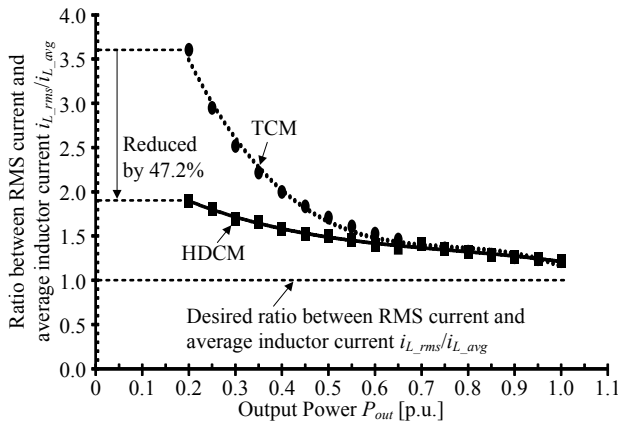


(a) Step-up HDCM current response (0.2 p.u. to 0.4 p.u.).

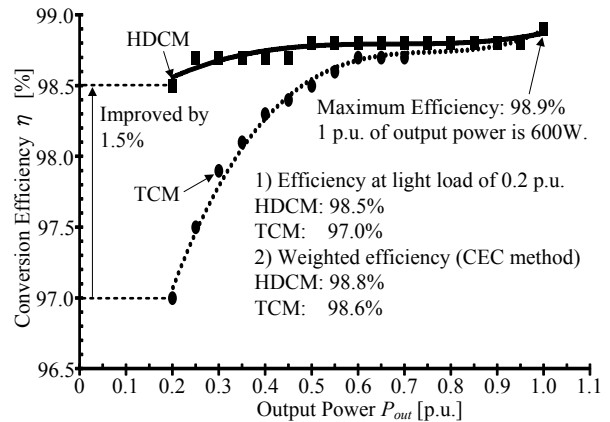


(b) Step-down HDCM current response (0.4 p.u. to 0.2 p.u.).

Fig. 12. Current response of HDCM. By controlling the positive and negative values of the TCM current, the average current of HDCM is controlled as same as DCM, which has been research thoroughly. However, the control frequency is required to be the same as the switching frequency in order to eliminate completely the small oscillation in the average current.



(a) Ratio between RMS current and average current of TCM and HDCM.



(b) Efficiency characteristic of TCM and HDCM.

Fig. 13. Comparison of RMS current and efficiency between TCM and HDCM. In HDCM, by flowing the TCM current during the zero-current interval of DCM, both ZVS and the current ripple reduction at light load are achieved without any additional components. In particular, the ratio between the RMS current  $i_{L\_rms}$  and the average inductor current  $i_{L\_avg}$  in the HDCM operation is reduced by 47.2% at most compared to the TCM operation. Consequently, the HDCM efficiency at light load of 0.2 p.u. is improved by 1.5%.

100 kHz. When the switching frequency is further increased, the high weighted efficiency can still be maintained by optimizing the snubber capacitor, which is used to reduce the turn-off loss, and the TCM current peak, which is designed to achieve ZVS.

Fig. 14 shows the advantages of the soft switching in HDCM and TCM over the hard switching in CCM. In the CCM operation, the hard switching leads to the occurrence of false triggering due to the high di/dt of the current. Two factors which increases significantly the di/dt of the current during the hard switching are as follows; the recovery current of the free-wheeling diode and the discharge current of the junction capacitor. In order to avoid the occurrence of the false triggering during the hard switching in CCM, the main circuit and the gate driver circuit are required to be customized for the high di/dt of the current, which is undesirable due to the increase in cost. Consequently, the soft switching in HDCM and TCM not only reduces the switching loss but also benefits the design cost of the main circuit and the gate driver circuit.

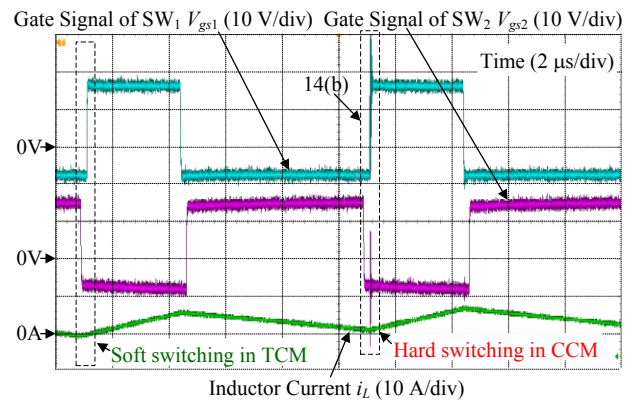
## V. CONCLUSION

This paper proposed a hybrid current mode between DCM and TCM, which was entitled Hybrid Discontinuous Current Mode, i.e. HDCM. In the HDCM operation, by applying the TCM operation into the zero-current interval of DCM, ZVS was achieved for all the switches without any modification of the main circuit. Furthermore, the total charge during the additional TCM interval was neutralized in order to have no influence on the DCM operation. This enabled the current ripple be reduced at light load in order to maintain the high efficiency at wide load range. In particular, compared to the TCM operation, the RMS current at light load of 0.2 p.u. was reduced by 47.2% with the application of HDCM. Consequently, the efficiency of HDCM was improved by 1.5% at most compared to TCM.

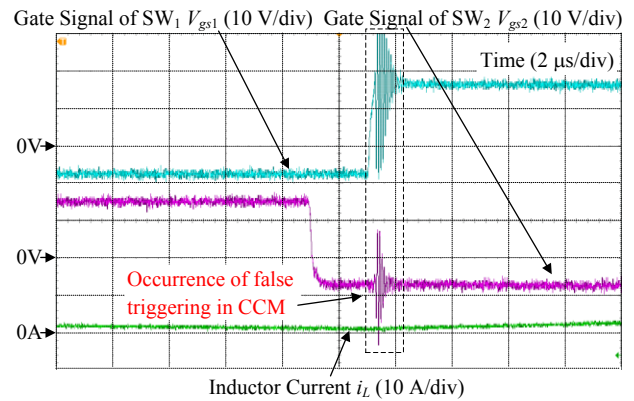
In the future works, the application of HDCM in other converters, e.g. the single-phase inverter and the three-phase inverter, will be presented.

## REFERENCES

- [1] Y. Lei, Ch. Barth, Sh. Qin, W. Liu, I. Moon, A. Stillwell, D. Chou, Th. Foulkes, Z. Ye, Z. Liao, R. C.N. Pilawa-Podgurski, "A 2 kW, single-phase, 7-level, GaN inverter with an active energy buffer achieving 216 W/in<sup>3</sup> power density and 97.6% peak efficiency", IEEE Applied Power Elec. Conf. and Ex. (APEC), pp. 1512-1519, 2016.
- [2] Y. Chen, Sh. Shiu, R. Liang, "Analysis and Design of a Zero-Voltage-Switching and Zero-Current-Switching Interleaved Boost Converter", IEEE Transactions on Power Electronics, Vol. 27, No. 1, pp. 161-173, 2012.
- [3] R. C. N. Pilawa-Podgurski, A. D. Sagneri, J. M. Rivas, D. I. Anderson, D. J. Perreault, "Very-High-Frequency Resonant Boost Converters", IEEE Transactions on Power Electronics, Vol. 24, No. 6, pp. 1654-1665, 2009.
- [4] J. Xue, H. Lee, "A 2-MHz 60-W Zero-Voltage-Switching Synchronous Noninverting Buck-Boost Converter With Reduced Component Values", IEEE Transactions on Circuits and Systems II: Express Briefs, Vol. 62, No. 7, pp. 716-720, 2015.
- [5] Junhong Zhang, Jih-Sheng Lai, Rae-Young Kim, Wensong Yu, "High-Power Density Design of a Soft-Switching High-Power



(a) Soft switching in TCM and hard switching in CCM.



(b) Occurrence of false triggering in CCM due to hard switching.

Fig. 14. Advantages of soft switching in HDCM and TCM over hard switching in CCM. In the CCM operation, the hard switching not only increases the switching losses but also leads to the occurrence of false triggering. In particular, the recovery current of the free-wheeling diode combining with the discharge current of the junction capacitor at the turn-on results in the high di/dt of the current.

- Bidirectional dc-dc Converter", IEEE Transaction on Power Electronics, Vol. 22, No. 4, pp. 1145 - 1153 (2007).
- [6] Christoph Marxgut, Florian Krismer, Dominik Bortis, Johann W. Kolar, "Ultraflat Interleaved Triangular Current Mode (TCM) Single-Phase PFC Rectifier", IEEE Transaction on Power Electronics, Vol. 29, No. 2, pp. 873 - 882 (2014).
- [7] Xiucheng Huang, Fred C. Lee, Qiang Li, Weijing Du, "High-Frequency High-Efficiency GaN-Based Interleaved CRM Bidirectional Buck/Boost Converter with Inverse Coupled Inductor", IEEE Transaction on Power Electronics, Vol. 31, No. 6, pp. 4343 - 4352 (2015).
- [8] Jian Sun, Daniel M. Mitchell, Matthew F. Greuel, Philip T. Krein, Richard M. Bass: "Averaged Modeling of PWM Converters Operating in Discontinuous Conduction Mode", Transactions on Power Electronics Vol.16, No. 4, pp.482-492, 2001.
- [9] K. D. Gusseme, D. M. V. de Sype, A. P. V. den Bossche, J. A. Melkebeek, "Digitally Controlled Boost Power-Factor-Correction Converters Operating in Both Continuous and Discontinuous Conduction Mode", IEEE Transactions on Power Electronics, Vol. 52, No. 1, pp. 88-97, 2005.
- [10] Sh. F. Lim, A. M. Khambadkone, "A Simple Digital DCM Control Scheme for Boost PFC Operating in Both CCM and DCM", IEEE Trans. on Power Electronics, Vol. 47, No. 4, pp. 1802-1812, 2011.
- [11] H. N. Le, D. Sato, K. Orikawa, J. Itoh, "Efficiency Improvement at Light Load in Bidirectional DC-DC Converter by Utilizing Discontinuous Current Mode", IEEE 17th European Conf. on Power Elec. and Applications (EPE'15-ECCE Europe), pp. 1-10, 2015.